Strathprints Institutional Repository

SMART MATERIALS APPLICATION ON HIGH PERFORMANCE SAILING YACHTS FOR ENERGY HARVESTING

S. Turkmen, D. Mylonas and **M. Khorasanchi,** University of Strathclyde, Glasgow, UK
Serkan.turkmen@strath.ac.uk, dimitrios.mylonas@strath.ac.uk, mahdi.khorasanchi@strath.ac.uk

Piezoelectric patches are bounded on a keel bulb in order to harvest vibration energy by converting electrical output. Unsteady computational fluid dynamics method is also used to find the structural boundary condition such as the hydrodynamic pressure fluctuation. Finite element analysis (FEM) is used to find structural and electrical responses.

NOMENCLATURE

Sym	Definition	[Unit]
δ	Variation operator	
ε	The permittivity (IEEE std)	F/m or C/(m·V)
ε_o	Permittivity of vacuum (8.854E-12)	
ϕ	Voltage, electrical potential	V/m
ω	Frequency	rad/s
Ω	Surface, area	m^2
ρ	The mass density	kg/m^3
ϱ	Surface charge density	C/m^2
E	Electric field	V/m
F_P	Point force	N
F_V	Body force	N
F_Ω	Surface force	N
c	Mechanical stiffness (IEEE std)	N/m^2
[C]	Structural damping matrix	
d	Piezoelectric strain constants	C/N
D	Electric displacement field	C/m^2
H	Total potential energy or electric enthalpy	Joules
K	Kinetic energy	Joules
[M]	Mass matrix	kg
P	Power	Watts
Q	Total electrical charge	V/m^2
S	Strain (IEEE std)	m/m
t_1,t_2	Time	s
σ	Stress (IEEE std)	N/m^2
$\{u\}$	Displacement field vector	m
$\{\dot{u}\}$	Velocity field vector	m/s
W	Total virtual work	Joules
Z	Impedance	ohm

Superscripts

T	Values taken at constant stress (T=0)
s	Values taken at constant strain (S = 0)
E	Values taken at constant electric field (E=0)
T	Transpose of a matrix (Italic)

Subscripts

i,*j*	Strain or stress applied in the j-axis and the normal direction of the electrode is i-axis.

1. INTRODUCTION

Piezoelectric (and pyroelectric) materials are types of smart material made from ferroelectric crystals. Curie brothers discovered the piezoelectric effect in 1880. Knowing that the electrification is generated by mechanical pressure, they investigated in what direction pressure should be applied and from which crystal classes the effect is to be expected. One of the early applications was made by Paul Langevin to detect submarines. He used quart-steel sandwich transducers, which are called the Langevin-type transducer in ultrasonic engineering [1].

Piezoelectricity is an electromechanical phenomenon that couples the elastic (dynamic coupling) and electric (static coupling) fields. In operation, this phenomenon can be observed when a piezoelectric material is adopted in a noise-vibration system or a mechanical force/pressure, cyclic electric field is excited. This is called the direct piezoelectric effect. Conversely, if an electric charge or field is applied to the material then it is called converse piezoelectric effect [2]. This dual action of the material has become a tool for vibration control and energy sources for many applications, for instance sensors and actuators, frequency filters, or high-frequency ultrasonic transducers.

If this electric energy is consumed via a suitable resistor as Joule heat, mechanical noise vibration is significantly suppressed; that is, it acts as a passive damper. Power generation ability has been studied in the past years [3, 4]. Operating wireless electronic devices without a wired power source has become an issue so researchers mainly focus on output power, piezoelectric properties, complexity of the system and cost efficiency [5-8].

Studies show that smart materials or intelligent system concepts modify the structural properties without additional materials or mechanisms [9]. Lead Zirconate

Titane (PZT) is one of the piezoelectric materials that are used in both actuators and sensors. It is bonded to the surface of the base structure as a thin film or laminated [10, 11]

Applications of smart materials in sailing yachts are limited. Murayama et al. [12] and Shimada et al. [13] studied the structural health monitoring and damage detection of IACC yacht hull and keel through fiber-optic strain sensors. Shenoi et al. [14] give a review and status of smart materials use in the marine environment, and their potential for application in various fields.

In this study, the piezoelectric material PZT-5H is used to harvest the energy of the flow-induced vibration in a yacht keel. Two numerical approaches are used: computational fluid dynamics (CFD) to calculate the input excitation forces, and finite element analysis (FEM) to find structural and electrical responses. FFT analysis is done to find vortex shedding frequency (as a dominant frequency) over the keel. Estimate of output power is calculated when the piezoelectric plate is excited by a time-harmonic surface normal stress.

2. INTERACTION BETWEEN ELECTRICAL AND MECHANICAL SYSTEMS

Piezoelectricity may be explained as a linear interaction between electrical and mechanical systems. One of the differences in piezoelectric materials, which make them smart materials, is that material properties are not constant. Their values change with external mechanical loads (stress), electric field strength and temperature. Linear interaction between mechanical and electrical systems is presented in Figure 1. It is assumed the ambient temperature does not vary significantly so thermal properties are ignored in this study. The diagram helps to understand how mechanical and electrical properties are mediated by the different material constants [1, 15]. This shows the constitutive relationships and coupling coefficients in a linearly coupled system.

Electromechanical coupling between the elastic and the electric fields is demonstrated. In this figure, the rectangles indicate the intensive variables such as forces and the circles show the extensive variables such as displacements. Thus, the piezoelectric material characteristics are the elastic, dielectric, and piezoelectric tensor components [15].

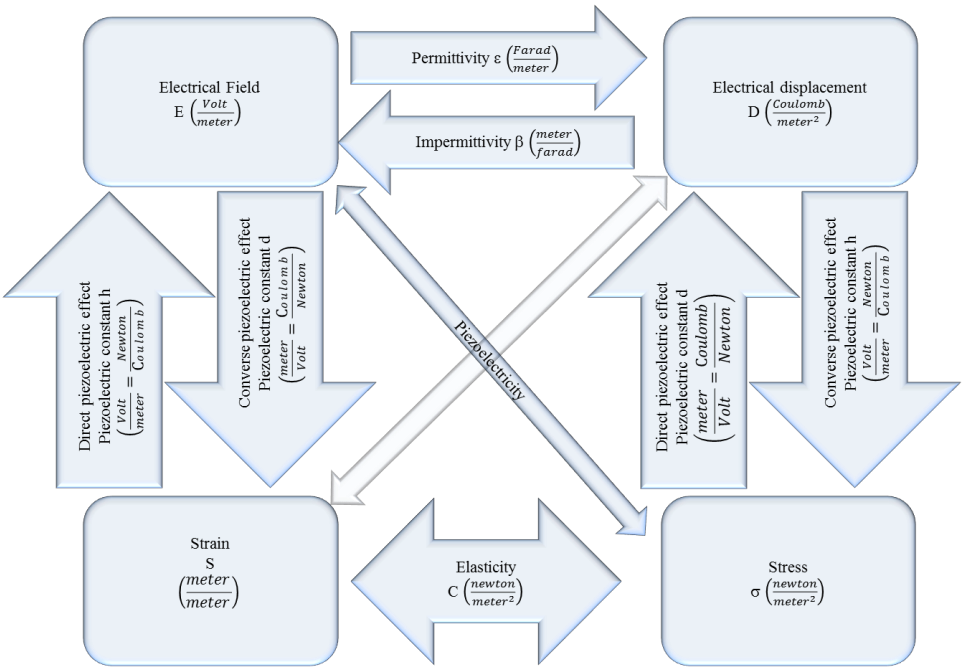

Figure 1 Piezoelectric effect

In Figure 1, mechanical quantities are $\{\sigma\}$ is the stress; $\{S\}$ is the strain; $[c]$ is the elastic stiffness matrix (forth-order tensor of elasticity coefficients); and electrical quantities are $\{E\}$ is the electric field; $\{D\}$ is the electric flux density vector; e is the piezoelectric tensor; $[\varepsilon]$ is the dielectric matrix at constant mechanical strain, d is the piezoelectric strain constant matrix.

The piezoelectric strain constants d_{ij} describe how much of the electric charge flows through short circuit when the force generating strain is applied to the piezoelectric material. In the other words, it is the ratio of charge density to applied mechanical strain:

$$d_{ij} = k_{ij}\sqrt{\varepsilon_{ii}^{T} s_{jj}^{E}} \qquad 1$$

Where, k_{ij} is the electromechanical coupling factor. It is a material constant which shows effectiveness of energy conversion between mechanical and electrical energy. There are three different factors depend on the actuation mode:

1. Thickness mode k_{33}
2. In-plane mode k_{31}=k_{32}
3. Shear mode k_{15}=k_{24}

Then dielectric matrix can be given by substituting those electromechanical coupling factors which are:

$$d_{31} = k_{31}\sqrt{\varepsilon_{33}^{T} s_{11}^{E}} \quad 2$$

$$d_{33} = k_{33}\sqrt{\varepsilon_{33}^{T} s_{33}^{E}} \quad 3$$

$$d_{15} = k_{15}\sqrt{\varepsilon_{11}^{T} s_{55}^{E}} \quad 4$$

2.1 GOVERNING EQUATIONS AND FINITE ELEMENT FORMULATION

Very often the solutions to these mathematical problems are complicated. The behaviours of the system cannot be seen explicitly and directly from the solutions; and numerical calculations have to be made for further examination of the system.
Hamilton's principle is used for theoretical derivations of the piezoelectric material governing equations of motion [2].

$$\delta \int_{t_1}^{t_2} (K - H + W)dt = 0 \quad 5$$

Here, K is the kinetic energy and H is the total potential energy. Kinetic energy and electric enthalpy function are called Lagrangian work L. W is the virtual work; δ denotes the variation; t_2 and t_1 are starting and finishing time, respectively. The total kinetic energy K for volume V of the piezoelectric material is [16]:

$$K = \frac{1}{2}\int_{\mathrm{V}} \dot{u}^{T} \rho \dot{u}\, d\mathrm{V} \quad 6$$

Where, $\dot{u}$ is the velocity field vector and ρ is the mass density. The potential energy H includes mechanical strain and electrical potential energies. It is also called the electric enthalpy:

$$H = \frac{1}{2}\int_{\mathrm{V}} \left(\sigma_{ij}^{T} S_{ij} - E_{i}^{T} D_{i}\right) d\mathrm{V} \quad 7$$

Where, σ^{T} is the stress tensor; S is strain tensor; E is the electrical field vector and D is the electric displacement or induction vector. The total virtual work W done by the external mechanical and electrical forces on the domain boundary $\partial\Omega$ is:

$$\delta W = \int_{\partial \mathrm{V}} T_i \delta u_i \, dV + \int_{\partial\Omega} \varrho \delta\phi \, ds \quad 8$$

Where T_i is the surface traction (=$\sigma_{ij}n_i$); ϱ is the surface electrical charge (=$D_i n_i$) on the domain boundary $\partial\Omega$ and Φ is the electrical potential.
The linear piezoelectric enthalpy function is written as [2]:

$$H(S_{kl}, E_i) = \frac{1}{2}\{S_{kl}\}^{T}[c]\{S_{kl}\} - \{S_{kl}\}^{T}[e]^{T}\{E_k\} - \frac{1}{2}\{E_{kl}\}^{T}[\varepsilon]\{E_{kl}\} \quad 9$$

Here, [c] is the elasticity coefficients matrix measured at a constant electric field; [e] is the piezoelectric constant matrix; [ε] is the dielectric constant matrix measured at a constant strain. It is assumed that isothermal process, thermo-mechanical coupling and pyroelectric effects are negligible.

The piezoelectric constitutive equations for the stress σ and the electric displacement D are derived from the enthalpy function. These equations were standardized in 1988 by IEEE association [17]. The linear piezoelectric relation of a piezoelectric continuum at a constant temperature and independent variable S and E is given as:

$$\{\sigma_{ij}\} = [c_{ijkl}{}^{E}]\{S_{kl}\} - [e_{kij}]\{E_k\} \quad 10$$

$$\{D_i\} = [e_{ikl}]\{S_{kl}\} + [\varepsilon_{ik}{}^{S}]\{E_k\} \quad 11$$

The stress tensor $\{\sigma_{ij}\}$ has two effects, mechanical and electrical. The first equation above denotes the converse piezoelectric effect and the second is the direct piezoelectric effect. In the linear piezoelectric constitutive equations, electrical field vector E is related to the electric potential field Φ given as:

$$E_k = -\phi_{,k} \quad 12$$

The strain tensor S_{kl} is given as:

$$\mathrm{S_{kl}} = \frac{1}{2}\left(\mathrm{u_{k,l}} + \mathrm{u_{l,k}}\right) \quad 13$$

An alternate formulation of the linear piezoelectric constitutive equations can be obtained when different independent variables, i.e. σ and E, are chosen such as:

$$S_{kl} = s_{ijkl}{}^{E}\sigma_{ij} + d_{kij}\,E_k \quad (14)$$

$$D_i = d_{ikl}\sigma_{ij} + \varepsilon_{ik}{}^{T}E_k \quad (15)$$

The virtual work W done by external mechanical and electrical loads is then given as [2]:

$$\delta W = \int_V \{\delta u\}^T\{F_V\}dV + \int_{\Omega s} \{\delta u\}^T\{F_\Omega\}\,\Omega + \{\delta u\}^T\{F_P\} - \int_{\Omega\phi} \delta\phi\varrho d\Omega - \delta\phi Q \quad (16)$$

Where, $\{F_V\}$, $\{F_\Omega\}$ and $\{F_P\}$ are the body, surface and the point load vectors, respectively. ϕ is the electrical potential; ϱ is the surface charge density; Q is the total charge on the surfaces. Ωs is the external mechanical loading surface, and $\Omega\phi$ is the external electrical loading surface.

By taking the constitutive equations into account and substituting the other parameters, Hamilton's principle yields the governing equations of motion in variational form [18]:

$$\begin{aligned} -\int_V [\rho[\delta\dot{u}]^T[\dot{u}] - \{\delta S\}^T[c^E]\{S\} + \{\delta S\}^T[e^E]^T\{E\} \\ + \{\delta E\}^T[c^E]\{S\} \\ + \{\delta E\}^T[\varepsilon^S]\{E\} \\ + \{\delta u\}^T\{F_V\}]dV \\ + \int_{\Omega s} \{\delta u\}^T\{F_\Omega\}\,d\Omega \\ + \{\delta u\}^T\{F_P\} \\ - \int_{\Omega\phi} \delta\phi\varrho d\Omega - \delta\phi Q = 0 \end{aligned} \quad (17)$$

The mechanical displacement $[u]$ and electric potential field ϕ are unknown functions. Hence, Finite element method is used to calculate these variables. To define finite element formulation the displacement is related to corresponding node values by the mean of the shape function. Similarly, the strain field and the electrical field are related to nodal displacements and potential by shape functions derivatives.

The elementary matrix form of governing equations can be obtained by substituting the nodal values into the above equations.

$$\begin{bmatrix} M & 0 \\ 0 & 0 \end{bmatrix}\begin{Bmatrix} \ddot{u} \\ 0 \end{Bmatrix} + \begin{bmatrix} C^U & 0 \\ 0 & 0 \end{bmatrix}\begin{Bmatrix} \dot{u} \\ 0 \end{Bmatrix} + \begin{bmatrix} K^u & K^z \\ K^{zT} & K^V \end{bmatrix}\begin{Bmatrix} u \\ V \end{Bmatrix} = \begin{Bmatrix} F \\ Q \end{Bmatrix} \quad (18)$$

Here, $[M]$ is the mass matrix; $[C^u]$ is the mechanical damping matrix; $[K^u]$ is the mechanical stiffness ; $\{u\}$ is the displacement vector; $\{F\}$ is the external force vector. $[K^Z]$ is the piezoelectric coupling matrix which contains piezoelectric constants in either $[d]$ form (strain/electric field) or $[e]$ form (stress/electric field); $[K^V]$ is the dielectric permittivity matrix; V is the electric voltage vector; and $\{Q\}$ is the externally applied charge vector.

3. BOUNDARY CONDITION DEFINITION

An America's Cup Keel developed by Werner et al under the version 5 of the IACC rules is used for the numerical study [12, 19]. Mylonas and Sayer presented the forces acting on the keel model [20]. A good accuracy has been found between CFD results and the experimental results. Different keel bulb configurations were used such as with winglets in different location on the bulb and no winglet in their study. In this study, no winglet configuration was chosen.

Pressure fluctuations on the surface are due to the vortices being shed from the body. They may excite the structure to vibrate and generate acoustic sound [21]. The frequency of excitation force is equal to the vortex shedding frequency, which depends on the shape and size of the body, the velocity of the flow, the surface roughness and the turbulence of the flow.
The relation between vortex shedding frequency (f_s) and flow speed (U) is identified by the Strouhal number (St).

$$St = \frac{f_s c}{U} \quad (19)$$

where c is a characteristic length.

The commercial CFD package STAR-CCM+ was used to calculate the pressure distribution on the structure. A spectral analysis was performed on the results to find the vortex-shedding frequency. The frequency of pressure fluctuations was found in the range of 32-40 Hz. The corresponding Strouhal Number is in the range of 0.18-0.20 (Figure 2). This result is reasonable when compared with open literature [22, 23].

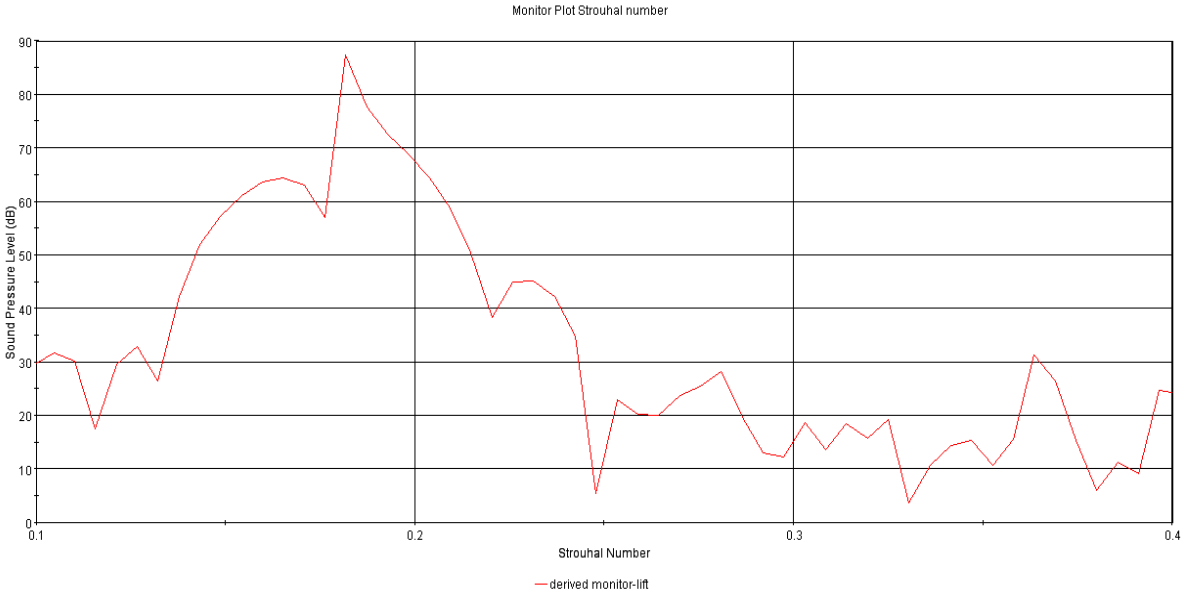

Figure 2 Sound Pressure Level derived from lifting force vs. Strouhal Number

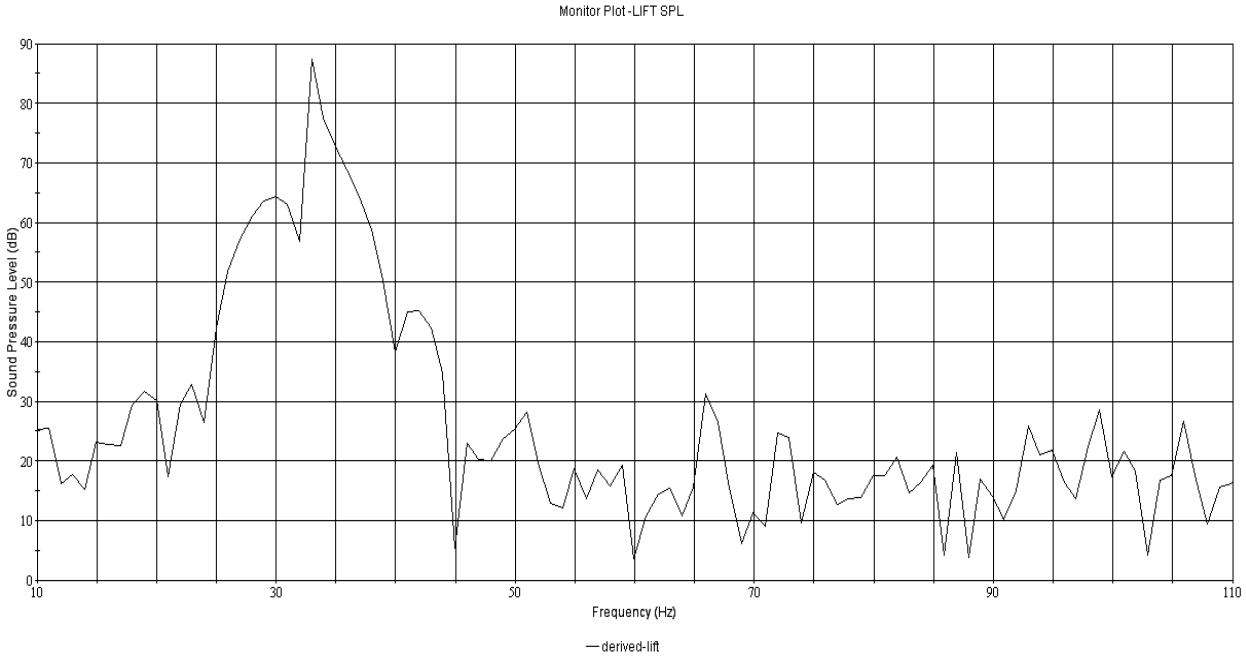

Figure 3 Sound Pressure Level derived from lifting force vs. Frequency

4. ENERGY HARVESTING FROM FLOW-INDUCED VIBRATION OF KEEL

The piezoelectric materials (PZT-5H plate element) are bounded on the port side and starboard side surfaces of the fin (Figure 4). The thickness h is 1 mm; the top and the bottom surface dimensions are 80x80mm. It is considered the PZT, poled in thickness direction (z or x_{33} axis), is excited by harmonic pressure (p). The finite element model is shown in Figure 4.The thickness of the fin is very thin compared with the base structure. Top and bottom surfaces are electrodes and are connected by a simple electrical circuit.

Although pressure that on the surface is imposing in thickness direction of surfaces total force is bending the structure. The piezoelectric material data should be set up by respect to actuation mode. The elastic compliance matrix s; the piezoelectric constant d; and the permittivity matrix ε are given for the PZT poled in the Z (or x_{33}) direction [24]:

$$[s] = \begin{bmatrix} s_{11} & s_{12} & s_{13} & 0 & 0 & 0 \\ s_{21} & s_{11} & s_{31} & 0 & 0 & 0 \\ s_{13} & s_{13} & s_{33} & 0 & 0 & 0 \\ 0 & 0 & 0 & s_{44} & 0 & 0 \\ 0 & 0 & 0 & 0 & s_{44} & 0 \\ 0 & 0 & 0 & 0 & 0 & s_{66} \end{bmatrix}$$

$$[d]^T = \begin{bmatrix} 0 & 0 & d_{31} \\ 0 & 0 & d_{31} \\ 0 & 0 & d_{33} \\ 0 & d_{15} & 0 \\ d_{15} & 0 & 0 \\ 0 & 0 & 0 \end{bmatrix};$$

$$[\varepsilon] = \begin{bmatrix} \varepsilon_{11} & 0 & 0 \\ 0 & \varepsilon_{11} & 0 \\ 0 & 0 & \varepsilon_{33} \end{bmatrix}$$

Here; s_{66}=2 (s_{11}-s_{12}); and the superscript "*T*" is matrix transpose. ε_0 is permittivity of free space. ρ is the mass density.

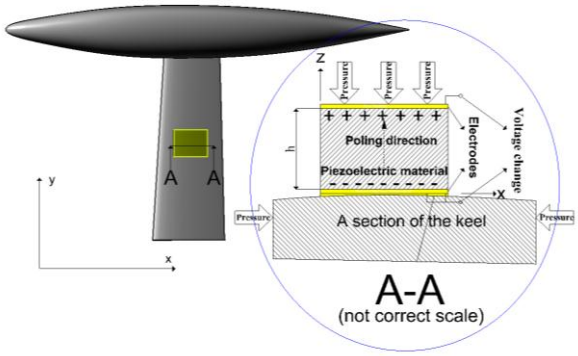

Figure 4 Physical model of the keel bulb bounded by the piezoelectric patches

4.1 STATIC ANALYSIS

At the beginning, a static analysis is performed to determine the static capacitance C_o. This value will be used to determinate the static impedance. Boundary conditions are determined as the top electrodes of the piezoelectric patch are applied 1V and bottom electrodes are grounded (V=0 volt).
As motion is time-harmonic, output power depends on the real part of impedance. The value is used to calculate impedance *Z*:

$$Z = \frac{1}{\omega C_o} \qquad 20$$

Here, ω is the rotational frequency (1/sec).

The major surfaces of the piezoelectric patch are electroded and a circuit with impedance *Z* (at time-harmonic motion) connects the electrodes.

4.2 MODAL ANALYSIS

Maximum benefit of the piezoelectric material can be obtained by installation at correct location with maximum strain. Therefore, the deformation due to pressure fluctuations of the surface is investigated before piezoelectric patch is added. It is expected to achieve higher output voltage at the natural frequency of the structure.

A modal analysis was carried out to estimate the natural frequencies of the structure without and with piezoelectric patch. Short circuit electrical boundary conditions are added for PZT bounded structure. In other words, top and bottom surfaces of piezoelectric materials are grounded (V=0 Volt). The results are given in Table 1.

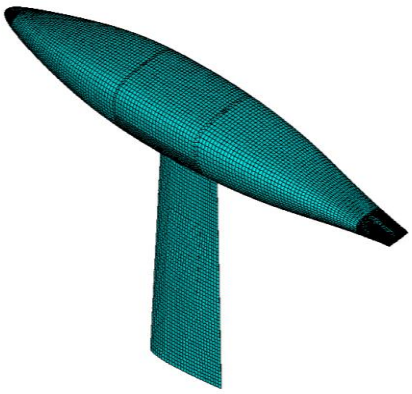

Figure 5 Finite element model of keel bulb bounded by the piezoelectric patch

Table 1 Comparison between the natural frequencies for the keel Bulb vs. the keel Bulb bounded piezoelectric material

Mode No	Frequency (Hz)	Frequency with PZT (Hz)
1	1.3897	1.5346
2	2.4272	2.7031
3	9.3596	9.4822
4	16.917	16.752
5	36.571	35.79
6	74.073	79.934
7	80.299	82.15

The mode shape gives preliminary idea about the location that piezoelectric material should be laminated on the structure. The result in Table 1 shows the natural frequency can be shifted when electrical load on the piezoelectric structure is controlled.

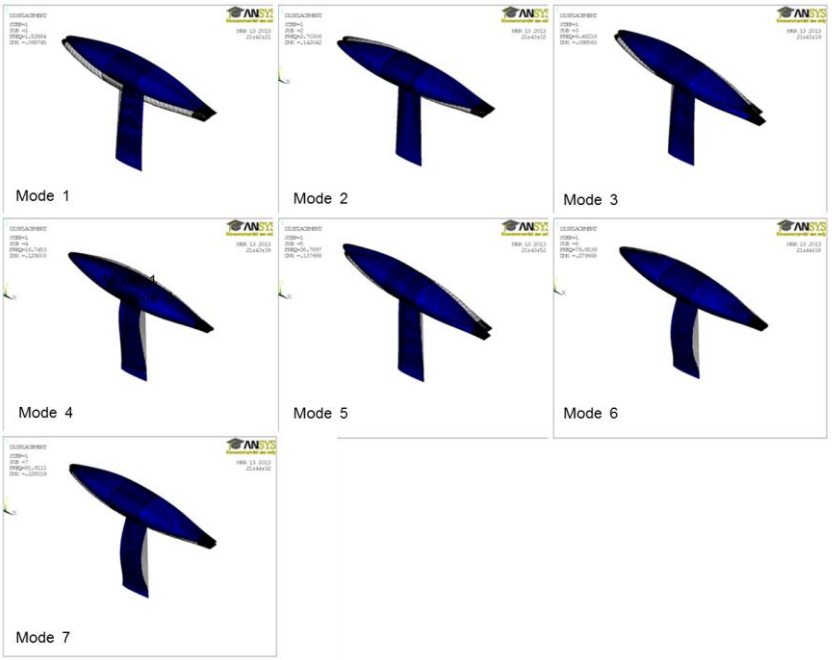

Figure 6 Mode Shapes of the keel bulb

4.3 HARMONIC ANALYSIS

A harmonic analysis was performed to find the charge on the electrodes of piezoelectric patch at a frequency around the range of vortex shedding frequency. The structure is excited by the flow and the response is in the form of electrical output. It is expected to find higher output at the natural frequency of the structure. As motion is time-harmonic, output power depends on the real part of impedance.

The average output electrical power per unit plate area over a period is [25]:

$$P_2 = \frac{1}{2}|\bar{I}|^2 Re\{Z\} \qquad 21$$

The result of output voltage is given in Figure 7. Although dominant frequency due to the vortex shedding is around 35 Hz, it is clear that the material develop higher voltage at structure's natural frequencies.

Mechanical input power (P_1) can be calculated by using velocity $\dot{u}_3$ which is in the z (x_{33}) axis and at the surfaces:

$$P_1 = \frac{1}{2}p(\dot{u}_3^* + \dot{u}_3) = pRe\{\dot{u}_3\} \qquad 22$$

The asterisk represents a complex conjugate. The efficiency of the piezoelectric harvester is the ratio of output power and input power.

$$\eta = \frac{P_2}{P_1} \qquad 23$$

The efficiency of the system at different frequency is shown in Figure 8. The efficiency is proportional to excitation frequency. An abnormal behaviour is observed in the plot. It might be due to static definition of impedance in a dynamic problem.

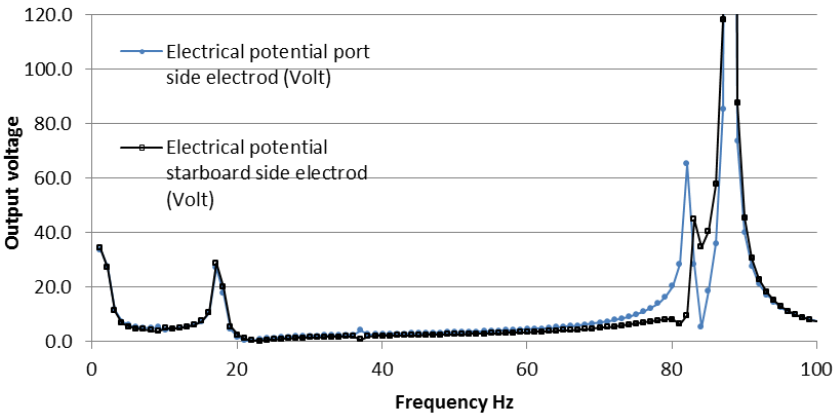

Figure 7 Output voltage versus frequency

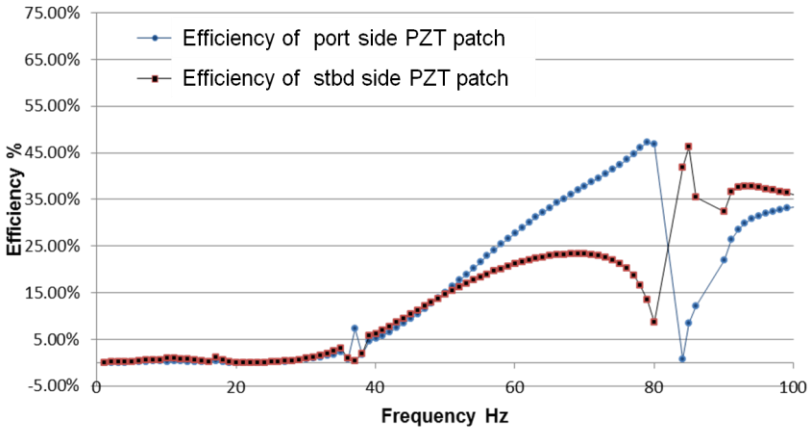

Figure 8 Efficiency of generating power

5. CONCLUSIONS

The present study proposed a new concept into the sailing and marine industry to save energy by harvesting unused (waste) vibration energy due to the flow around the structure. It can be also called a technology transfer as this concept has been successfully applied for aerospace structures.

A piezoelectric patch was installed on the keel of a yacht. A CFD analysis was carried out to find the excitation force and the predominant frequency. Next, a finite element study was performed to investigate the response of the structure and the generated electricity by piezoelectric patch.

It was observed that the output power is dependent on real part of impedance which is resistance of piezoelectric material. It is expected that piezoelectric system is more efficient at higher frequencies.

Piezoelectric effect occurs under stress and the direction of the stress. Flow pressure generates load in the thickness direction, however total pressure deforms the structure. The type of forces on the piezoelectric patch is important for correct selection of piezoelectric material. If the dominant forces are imposed in the thickness direction then piezoelectric patch operates with thickness-stretch mode and the corresponding piezoelectric constant d_{ij} is the important property. Flow causes bending motions on the structure so piezoelectric material operates with thickness-shear modes. In this case the parameter d_{31} plays the significant role and must be considered.

It is also interesting to investigate this concept study applied to a mast and rigging structure (due to the bluff body nature of the mast), and even on sails in certain sailing conditions as it is expected the influence of the flow-induced vortex vibration to be more significant.

Future work will follow and will consist of experimentally investigating the piezoelectric effect of PZT bonded on a fin (Figure 9) or flat plate in a towing tank, with measurements of vibration, damping and electrical output, seconded by further numerical validation at full scale. A closed electric circuit will be attached to piezoelectric patch (called piezoelectric shunt damping system) in order to reduce vibration.

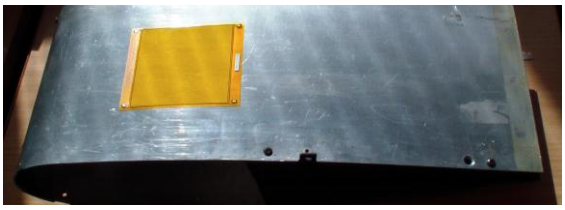

Figure 9 A piezoelectric patch on a test fin

6. ACKNOWLEDGEMENTS

The authors would like to thank Prof. O. Turan for bringing the idea and opportunity to study this topic, and Prof. S. Day for giving access to test facilities and equipment. The authors also acknowledge the experience and discussion shared with Mr. P. Zoet, CEO of PZDynamics. Finally, the authors are grateful to the faculty of engineering of Strathclyde University for providing access to HPC facilities.

7. REFERENCES

1. IKEDA, T., 'Fundamentals of piezoelectricity'. Oxford ; New York : *Oxford University Press*, 1996.
2. TZOU, H.S., 'Piezoelectric shells- Distributed sensing and control of continua'. Dordrecht, Netherlands: Kluwer Academic Publishers (*Solid Mechanics and Its Applications*) 19, 1993.
3. JIASHI, Y., HONGGANG, Z., and YUAMTAI, H., 'Performance of a Piezoelectric Harvester in Thickness--stretch Mode of a Plate'. *IEEE Transactions on Ultrasonics, Ferroelectrics, and Frequency Control*, 52(10): p. 1872-1876, 2005.
4. KONG, N., et al., 'Resistive impedance matching circuit for piezoelectric energy harvesting'. *Journal of Intelligent Material Systems and Structures*, 21(13): p. 1293-1302, 2010.
5. BADEL, A., et al., 'Single crystals and nonlinear process for outstanding vibration-powered electrical generators'. *IEEE transactions on ultrasonics, ferroelectrics, and frequency contro*l, 53(4): p. 673-684, 2006.
6. JI, H., et al., 'Semi-active vibration control of a composite beam by adaptive synchronized switching on voltage sources based on LMS algorithm'. *Journal of Intelligent Material Systems and Structures*, 20(8): p. 939-947, 2009.
7. RAKBAMRUNG, P., et al., 'Performance comparison of PZT and PMN–PT piezoceramics for vibration energy harvesting using standard or nonlinear approach'. *Sensors and Actuators* A: Physical, 163(2): p. 493-500, 2010.
8. BADEL, A., et al., 'Piezoelectric vibration control by synchronized switching on adaptive voltage sources: Towards wideband semi-active damping'. *The Journal of the Acoustical Society of America*, 119: p. 2815, 2006.
9. SCHMIT, L.A. and FARSHI, B., 'Optimum laminate design for strength and stiffness'. *International Journal for Numerical Methods in Engineering*, 7(4): p. 519-536, 1973.
10. HWANG, W.-S. and PARK, H.C., 'Finite element modeling of piezoelectric sensors and actuators'. *AIAA journal*, 31(5): p. 930-937, 1993.
11. KUMAR, N. and SINGH, S.P., 'Vibration control of curved panel using smart damping'. *Mechanical Systems and Signal Processing*, 30: p. 232-247, 2012.
12. WERNER, S., 'Computational hydrodynamics applied to an America's Cup class keel-best practice and validation of methods'. *Chalmers University of Technology*, 2006.
13. SHIMADA, A., et al., 'Damage Detection for International America's Cup Class Yachts Using a Fiber Optic Distributed Strain Sensor'. *IEICE transactions on electronics*, 86(2): p. 218-223, 2003.
14. SHENOI, A., WADDAMS, A., and SINHA, A., 'Smart Materials in the Marine Environment – a State of the Art Review', A.W. Ajit Shenoi, Ashutosh Sinha, Editor, *Materials Knowledge Transfer Network (KTN)*, 2009.
15. HEYWANG, W., LUBITZ, K., and WERSING, W., 'Piezoelectricity: Evolution and Future of a Technology'. Vol. 114, *Springer Verlag*, 2008.
16. TZOU, H. and TSENG, C., 'Distributed vibration control and identification of coupled elastic/piezoelectric systems: finite element formulation and applications'. Mechanical *Systems and Signal Processing*, 5(3): p. 215-231, 1991.
17. MEITZLER, A., et al., 'IEEE standard on piezoelectricity'. *IEEE*, New York, 1988.
18. PIEFORT, V., 'Finite element modelling of piezoelectric active structures', *Université Libre de Bruxelles*, 2001.
19. WERNER, S., et al., 'Computational fluid dynamics validation for a fin/bulb/winglet keel

configuration'. *Journal of Ship Research*, 51(4): p. 343-356, 2007.
20. MYLONAS, D. and SAYER, P., 'The hydrodynamic flow around a yacht keel based on LES and DES'. *Ocean Engineering*, 46(0): p. 18-32, 2012.
21. BLEVINS, R.D., 'Flow-induced vibration'. *Van Nostrand Reinhold Co.*, Inc, New York, 1990.
22. KRYLOV, V.V. and PORTEOUS, E. , 'Wave-like aquatic propulsion of mono-hull marine vessels'. *Ocean Engineering*, 37(4): p. 378-386, 2010.
23. TAYLOR, G.K., NUDDS, R.L., and THOMAS, A.L.R., 'Flying and swimming animals cruise at a Strouhal number tuned for high power efficiency'. *Nature*, 425(6959): p. 707-711, 2003.
24. XIE, J., et al., 'A piezoelectric energy harvester based on flow-induced flexural vibration of a circular cylinder'. *Journal of Intelligent Material Systems and Structures*, 23(2): p. 135-139, 2012.
25. YANG, J., 'Analysis of piezoelectric devices'. *World Scientific*, 2006.

AUTHORS BIOGRAPHY

S. Turkmen is a PhD student in the Department of Naval Architecture and Marine Engineering, University of Strathclyde, Glasgow. He has been researching on the topic of smart material application to mitigate noise and vibration in ships. He is also investigating underwater-radiated noise due to the cavitating propellers.

D. Mylonas has recently completed his PhD in the Department of Naval Architecture and Marine Engineering, University of Strathclyde, Glasgow. His research topic focused on the application of LES and DES in yacht hydrodynamics. He also holds an M.Eng from the same department. Other interests include ship & marine hydrodynamics, smart materials, yacht design and CFD simulations on marine and aerodynamic applications.

M. Khorasanchi is a research fellow in the Department of Naval Architecture and Marine Engineering, University of Strathclyde, Glasgow. Dr Khorasanchi has carried out several studies on vortex-induced-vibration (VIV) of marine risers and VIV suppression devices. His current teaching and research interests centre on hydrodynamics and marine propulsion. He investigates the hydrodynamic performance of marine vessels through full-scale CFD simulation. He also works on retrofitting technologies to improve the performance of marine vessels and reduce the fuel consumption and carbon emission of shipping industry.